Journal of Human Genetics (2013) 58, 428–433

www.nature.com/jhg

REVIEW

# Clinical application of the CpG island methylator phenotype to prognostic diagnosis in neuroblastomas

Kiyoshi Asada, Masanobu Abe and Toshikazu Ushijima

**Clinical applications of aberrant DNA methylation to cancer diagnostics and therapeutics are accelerating. Especially, the CpG island methylator phenotype (CIMP), simultaneous methylation of multiple genes, provides information that cannot be obtained by other diagnostic methods and therapeutic opportunities. CIMP is known to be associated with poor or good prognosis depending upon cancer types. We identified that CIMP in neuroblastomas (NBLs) is strongly associated with poor prognosis in Japanese NBL cases (hazard ratio (HR) = 22). Almost all NBLs with *MYCN* amplification displayed CIMP, and even among NBLs without *MYCN* amplification, NBLs with CIMP had worse prognosis (HR = 12). The prognostic power was faithfully reproduced in German NBL cases by the same methods, and also in Italian and Swedish NBL cases with different analytical methods. Mechanistically, methylation silencing of different sets of tumor-suppressor genes is involved in poor prognosis of NBLs with CIMP, and the presence of CIMP is most sensitively detected by methylation of the *PCDHB* family. For therapeutic purposes, a combination of 5-aza-2′-deoxycytidine, a DNA-demethylating drug, with 13-*cis*-retinoic acid, a differentiating drug, has been shown to be effective for NBLs *in vitro*, and further development of a better combination(s) is awaited. Now, epigenetic diagnosis and therapeutics are becoming or have become an important choice for cancer patients.**
*Journal of Human Genetics* (2013) **58**, 428–433; doi:10.1038/jhg.2013.64; published online 6 June 2013

**Keywords:** CIMP; neuroblastoma; poor prognosis

## INTRODUCTION

Aberrant DNA methylation is inherited over cell divisions and is deeply involved in carcinogenesis. Increasing numbers of cancer-specific aberrant methylation have been identified, and their usefulness in cancer diagnostics is becoming clear. DNA-demethylating drugs have been developed, and their usefulness in cancer therapeutics is also becoming clear. In cancer diagnostics, methylation of the Septin-9 gene in plasma is now being clinically evaluated as a detection marker for colorectal cancers.[1] Methylation of $O^6$-methylguanine-DNA methyltransferase in glioblastoma tissues is also used to predict the response of tumors to alkylating drugs.[2] Methylation of glutathione *S*-transferase pi1 specific to prostate cancer cells is used to detect the presence of prostate cancer in prostatectomy or biopsy tissue.[3] In addition to methylation of specific genes, the CpG island methylator phenotype (CIMP), methylation of multiple genes, has been reported to be associated with prognosis in various cancers.[4]

The therapeutic application of DNA methylation has already been brought into practice. Two demethylating drugs, 5-aza-2′-deoxycytidine (5-aza-CdR) and 5-azacytidine (5-aza-CR), have been approved by the US Food and Drug Administration for treatment of myelodysplastic syndrome. Application of these demethylating drugs to treatment of solid tumors is being tested in clinical trials.[5] In addition to these clinically used drugs, a new generation of DNA-demethylating drugs, such as SGI-110 and CP-4200, are also being developed.[6] Combinations of DNA-demethylating drugs with other drugs, such as histone deacetylase inhibitors,[7] cellular differentiating drugs[8] and cytotoxic drugs,[9] have produced some promising results.

In this review, we will introduce CIMP in various cancers and then focus on the high usefulness of CIMP in prognostic diagnosis of neuroblastomas (NBLs) and the potential in their treatment.

## CIMP IN VARIOUS CANCERS OTHER THAN NBLS

CIMP was originally established in colorectal cancers by the pioneering work of Toyota *et al*[10]. Some colorectal cancers had frequent DNA methylation of specific CpG islands and were associated with microsatellite instability. Colorectal cancers are now classified into three groups, CIMP-high (CIMP1, HME), CIMP-low (CIMP2, IME) and CIMP-0 (CIMP-negative, LME), using tumor-specific methylation markers.[11–13] CIMP-high cases show low mortality compared with CIMP-0 (hazard ratio (HR) = 0.44; 95% confidence interval (CI) = 0.22–0.88; $n = 649$)[11] (Table 1). CIMP-high, -low and -0 are strongly associated with mutations of *BRAF*, *KRAS* and *TP53*, respectively.[11,12] Although the cause–consequence relationship between oncogene mutations and CIMP has not been established, some investigators propose that methylation silencing of senescence pathways is necessary to suppress oncogene-induced senescence and for a cell with an oncogene mutation to survive.[14,15]

Division of Epigenomics, National Cancer Center Research Institute, Tokyo, Japan
Correspondence: Dr T Ushijima, Division of Epigenomics, National Cancer Center Research Institute, 1-1 Tsukiji 5-chome, Chuo-ku, Tokyo 104-0045, Japan.
E-mail: tushijim@ncc.go.jp
Received 24 April 2013; revised 6 May 2013; accepted 11 May 2013; published online 6 June 2013

**Table 1 CIMP in various cancers and association with prognosis**

| | *CIMP markers* | | | |
|---|---|---|---|---|
| *Cancer type* | *Original markers* | *Other markers* | *Prognosis of patients with CIMP* | *Reference* |
| Colorectal cancer | MINT27, MINT2, MINT1, MINT12, MINT17, MINT31, MINT25 | None | NA | 10 |
| Colorectal cancer | None | *CACNA1G, IGF2, NEUROG1, RUNX3, SOCS1* | NA | 50 |
| Colorectal cancer | MINT27, MINT2, MINT1, MINT12, MINT17, MINT31 | *p16, p16ex1, hMLH1, RASSF1A, DAPK, MGMT, TIMP3, ER, sFRP1, MyoD1, HPP1, hTERT, RIZ1, p14, Megalin, COX2, THBS1, THBS2, SOCS1, RUNX3, Neurog1* | NA | 12 |
| Colorectal cancer | None | *p16, hMLH1, CACNA1G, IGF2, NEUROG1, RUNX3, SOCS1, CRABP1* | Good CIMP-high vs -0 (HR = 0.44; 95% CI = 0.22–0.88; $n = 649$) | 11 |
| Colorectal cancer | MINT2, MINT1, MINT17, MINT31, | *p16, hMLH1, RASSF1A, MGMT, TIMP3, p14, CACNA1G, IGF2, NEUROG1, RUNX3, SOCS1, ALX4, RASSF5, ABTB2, C4orf31, CHFR, COL4A2, DUSP26, EFEMP1, IGFBP3, IGFBP7, IRF8, LOX, PPP1R3C, SCAM1, STOX2, TLE4, TMEFF2, UCHL1, ADAMTS1, AOX1, CDO1, CLDN23, EDIL3, EFHD1, ELMO1, EPHB1, FBN2, HAND1, ID4, KIAA0495, PENK, PPP1R14A, SSFRP1, SLC30A10, SPON1, THBD, TSPYL5, ZNF447, BNIP3, CIDEB, DFNA5, GRHL2, HLTF, OVOL1, RASSF2, TOLLIP* | NA | 13 |
| Gastric cancer | MINT2, MINT1, MINT12, MINT31, MINT25 | None | Good CIMP-high vs -negative, $P = 0.004$; CIMP-low vs -negative, $P = 0.012$; $n = 78$[25] | 16,17,25 |
| Lung cancer | MINT1, MINT31, MINT32 | *p16, MLH1, RASSF1A, RARβ, APC, DAPK, MGMT, GSTP1, CDH1, CDH13, sFRP1, sFRP2, sFRP4, sFRP5, TMS1, LAMC2* | NA | 18 |
| Liver cancer | MINT2, MINT1, MINT27, MINT31 | *p16, CACNA1G, COX2, ER* | NA | 19 |
| Ovarian cancer | None | 182 CGIs on a CGI microarray | Poor $P < 0.001$, $n = 19$ | 24 |
| Leukemia | None | *p16, DAPK, CDH1, CDH13, sFRP1, sFRP2, sFRP4, sFRP5, TMS1, FHIT, ADAMTS1, ADAMTS5, APAF1, ASPP1, DBC1, DIABLO, DKK3, HDPR1, hRFC, LATS1, LATS2, NES1, p14, p15, p57, p73, PACRG, PARK2, PTEN, REPRIMO, RIZ, SHP1, SMC1L1, SMC1L2, SYK, WIF1* | Poor $P = 0.04$, $n = 54$ | 21 |
| Bladder cancer | None | *p16, RASSF1A, RARβ, APC, DAPK, MGMT, GSTP1, CDH1, CDH13, FHIT* | Poor $P = 0.01$, $n = 98$ | 22 |
| Esophageal adenocarcinoma | None | *p16, APC, DAPK, MGMT, CDH1, TIMP3, ER* | Poor HR = 2.7; 95% CI = 1.1–6.5; $P = 0.02$; $n = 41$ | 23 |
| Glioblastoma | None | 1503 CpG sites on Infinium HumanMethylation450 bead array | Good $P = 0.017$, $n = 253$ | 26 |
| Glioblastoma | None | 9711 CpG sites on Infinium HumanMethylation450 bead array | Good $P < 0.001$, $n = 72$ | 27 |

Abbreviations: CI, confidence interval; CIMP, CpG island methylator phenotype; HR, hazard ratio; NA, not applicable.

The presence of CIMP has been reported in several other cancers, such as gastric,[16,17] lung,[18] liver,[19] ovarian cancers[20] and leukemias[21] (Table 1). The definition of CIMP is different in each cancer and the relationship between CIMP and prognosis is also different. Poor survival is associated with CIMP in bladder cancers ($P = 0.01$, $n = 98$),[22] esophageal adenocarcinomas (HR = 2.7; 95% CI = 1.1–6.5; $P = 0.02$; $n = 41$),[23] ovarian tumors ($P < 0.001$, $n = 19$)[24] and leukemias ($P = 0.04$, $n = 54$).[21] On the other hand, better survival is associated with CIMP in gastric cancers (CIMP-high vs -negative, $P = 0.004$, CIMP-low vs -negative, $P = 0.012$, $n = 78$).[25]

CIMP in glioblastomas is exceptionally well-characterized from a molecular viewpoint, and designated as G-CIMP. G-CIMP is associated with good prognosis ($P = 0.017$, $n = 253$),[26] and is known to be caused by isocitrate dehydrogenase 1 (*IDH1*) mutation.[27] Functionally, *IDH1* mutation has been shown as a gain-of-function mutation and to catalyze the NADPH-dependent reduction of α-ketoglutarate to 2-hydroxyglutarate.[28] 2-Hydroxyglutarate inhibits TET methylcytosine dioxygenase 2 that catalyzes the conversion of 5-methylcytosine to 5-hydroxymethylcytosine,[29] and the inhibition of TET is considered to lead to methylation of multiple genes. Similar to the association of *IDH1* mutation and G-CIMP, *IDH1/2* mutation is also associated with methylation patterns in AML.[30]

## IDENTIFICATION OF CIMP IN NBLS AS A STRONG PROGNOSTIC MARKER

NBL, derived from primitive cells of the sympathetic nervous system, is the most frequent extracranial cancer in childhood,[31] and is characterized by two extreme outcomes, spontaneous regression and

rapid progression. Accurate risk prediction is important for NBL in order to implement a necessary and sufficient level of treatment, and the International Neuroblastoma Risk Group classification system has been established for this purpose.[32] In this system, seven prognostic factors (stage, age, histologic category, grade of tumor differentiation, DNA ploidy and copy-number status at *MYCN* and at chromosome 11q) are used as the most clinically relevant factors. However, especially in the NBLs without *MYCN* amplification, it is still difficult to predict accurate prognosis and to decide on the therapeutic strategy.

Considering the major involvement of epigenetic machinery in embryonic development,[33,34] we searched for CGIs specifically methylated in NBLs with poor prognosis, not in those with good prognosis, using methylation-sensitive representational difference analysis.[35] Five CGI (or CGI groups), namely the *PCDHB* family, the *PCDHA* family, *HLP*, *DKFZp451I127* and *CYP26C1*, were found to be specifically methylated in NBLs with poor prognosis. Methylation of these five CGI (groups) was dependent upon each other, and conformed to the concept of CIMP. Methylation levels of the *PCDHB* family showed a clear bimodal distribution (Figure 1a), and NBL cases with high methylation levels of the *PCDHB* family showed poor overall survival with a HR of 22 (95% CI = 5.3–93) in 140 Japanese NBL cases.[35] Therefore, we decided to use the methylation levels of the *PCDHB* family as a marker of CIMP in NBLs.

To avoid false 'too good' results likely to be obtained by a genome-wide screening, we analyzed the prognostic power of CIMP in 152 German NBL cases in collaboration with Dr Schwab and Dr Westermann[36] (Figure 1b). DNA of German NBL cases was sent to our laboratory in Tokyo without clinical information, and methylation levels of the *PCDHB* family were analyzed. Regarding the cutoff value, as values between 40 and 60% gave high HRs in Japanese NBL cases, cases with methylation levels lower than 40% and higher than 60% were classified as NBLs without and with CIMP, respectively. The strong association between CIMP and poor overall survival was faithfully reproduced in German NBL cases with a HR of 9.5 (95% CI = 3.2–28). In addition, German NBL cases had information on disease-free survival, which was not available in Japanese NBL cases, and CIMP was shown to have prognostic significance also for disease-free survival with a HR of 5.4 (95% CI = 2.9–10). In addition to our studies, the strong prognostic power of CIMP was further confirmed in Italian and Swedish NBL cases.[37,38] Currently, in order to evaluate the clinical utility of CIMP as a prognostic marker, a prospective study is being conducted.

## COMPARISON OF CIMP WITH *MYCN* AMPLIFICATION

*MYCN* amplification is known as the strongest prognostic marker for NBLs and is one of the first molecular markers used in practice.[39–41] The presence of *MYCN* amplification is therefore used as a biomarker for stratification of NBLs in practice and trials. Importantly, almost all NBLs with *MYCN* amplification displayed CIMP (37/38 in Japanese and 23/23 in German NBL cases) while some NBLs without *MYCN* amplification also displayed CIMP[35,36] (Figure 2a). The cases with *MYCN* amplification showed poor overall survival with HR of 9.5

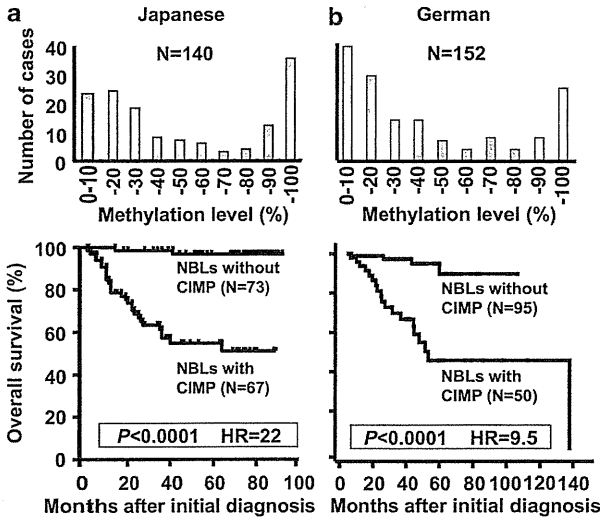


**Figure 1** Bimodal distribution of methylation levels of the *PCDHB* family and its association with survival. (**a**) In 140 Japanese neuroblastoma (NBL) cases, the methylation level of the *PCDHB* family showed bimodal distribution (modified from Abe *et al.*[35]). The cutoff value for *PCDHB* family was set at 40%. NBLs with CpG island methylator phenotype (CIMP) had significantly and markedly worse overall survival, analyzed by the Kaplan–Meier method. (**b**) In 152 German NBL cases, a similar bimodal distribution of the *PCDHB* family methylation level was observed. As cutoff values between 40 and 60% gave high HRs in Japanese NBL cases, before the analysis, cutoff values of 40 and 60% were set for cases without and with CIMP, respectively, and cases with intermediate values were classified as intermediate. It was reproduced that NBLs with CIMP had significantly and markedly worse overall survival (modified from Abe *et al.*[36]).

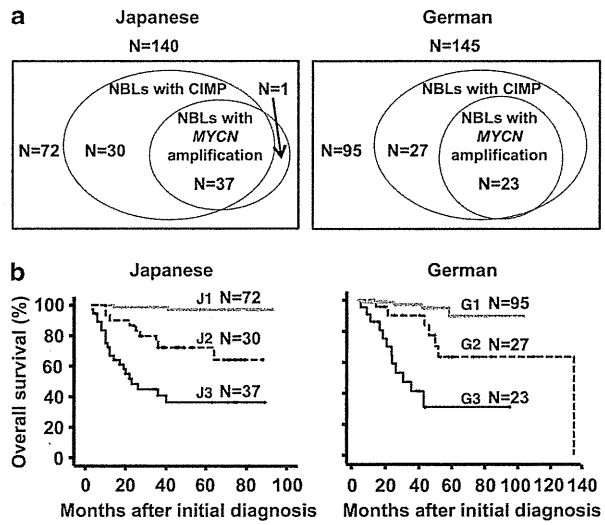


**Figure 2** Comparison of CpG island methylator phenotype (CIMP) and *MYCN* amplification. (**a**) The relationship between neuroblastomas (NBLs) with CIMP and those with *MYCN* amplification are shown by Venn diagrams. Almost all NBLs with *MYCN* amplification (37/38 in Japanese and 23/23 in German NBL cases) displayed CIMP, and some additional cases had CIMP only. (**b**) Kaplan–Meier analysis of (J1, G1) NBL cases without CIMP or *MYCN* amplification ($N=72$ in Japanese and $N=95$ in German NBL cases), (J2, G2) NBL cases with CIMP without *MYCN* amplification ($N=30$ in Japanese and $N=27$ in German NBL cases), (J3, G3) NBL cases with both CIMP and *MYCN* amplification ($N=37$ in Japanese and $N=23$ in German NBL cases). Among NBLs without *MYCN* amplification (J1, J2 in Japanese and G1, G2 in German NBL cases), CIMP also had a significant and strong prognostic marker with a hazard ratio of 12 (95% confidence interval (CI) = 2.6–59; $P=0.002$) in Japanese and 4.5 (95% CI = 1.3–16; $P=0.02$) in German NBL cases.

(95% CI = 4.4–21) and 12 (95% CI = 4.9–29) in Japanese and German NBL cases, respectively.[35,36] Therefore, NBL cases were classified into three groups: (J1) NBL cases without CIMP nor *MYCN* amplification ($N = 72$), (J2) NBL cases with CIMP without *MYCN* amplification ($N = 30$) and (J3) NBL cases with both CIMP and *MYCN* amplification ($N = 37$) in Japanese NBL cases. German NBL cases were also classified into three groups (G1–G3) in the same manner (Figure 2b). The three groups, respectively, showed step-wise increases of risk, and notably, among NBLs without *MYCN* amplification (J1, J2 in Japanese and G1, G2 in German NBL cases), NBLs with CIMP showed worse prognosis with a HR of 12 (95% CI = 2.6–59) in Japanese and 4.5 (95% CI = 1.3–16) in German NBL cases. The almost complete inclusion of NBLs with *MYCN* amplification in those with CIMP indicates that these two abnormalities are very closely associated with each other. However, it is still unknown whether CIMP causes *MYCN* amplification, *MYCN* amplification causes CIMP, these two must coexist for development of NBLs, or if there is a shared upstream event.

## MECHANISM FOR THE ASSOCIATION BETWEEN CIMP AND POOR PROGNOSIS

CGIs of the *PCDHB* family are located in their gene body, and their methylation was not associated with gene expression levels.[35] This suggested that, although methylation of the *PCDHB* family was closely associated with poor survival, simultaneous methylation of promoter CGIs was mechanistically involved in the poor survival (Figure 3). Indeed, in our study of Japanese NBL cases, methylation of promoter CGIs of the *RASSF1A, BLU, CYP26C1, FERD3L, CRYBA2* and *PCDHGC4* were methylated at significantly higher incidences in NBLs with CIMP, indicating that methylation silencing of tumor-suppressor genes was indeed associated with CIMP.[8,35]

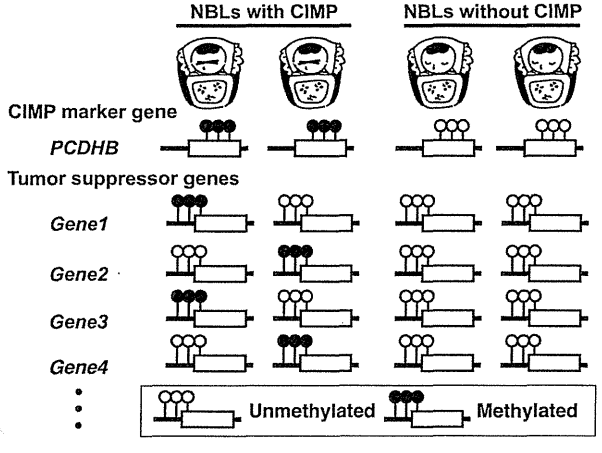


**Figure 3** A likely mechanism for the association between CpG island methylator phenotype (CIMP) and poor prognosis. In neuroblastomas (NBLs) with and without CIMP, the exonic CGIs of the *PCDHB* family and promoter CGIs of tumor-suppressor genes typically showed methylation statuses as in this scheme. NBLs with CIMP had methylation of the exonic CGIs of the *PCDHB* family consistently, and that of promoter CGIs of multiple tumor-suppressor genes with lower frequencies. Although methylation silencing of tumor-suppressor genes was considered to be responsible for the poor prognosis of NBLs with CIMP, methylation of individual genes had less sensitivity of CIMP than methylation of the *PCDHB* family. On the other hand, NBLs without CIMP did not have methylation of the exonic CGIs of the *PCDHB* family or that of promoter CGIs of tumor-suppressor genes, and thus were considered to have a good prognosis.

To strengthen this hypothesis, we further analyzed methylation of promoter CGIs of genes whose silencing was reported to be involved in development or progression of NBLs, namely *CASP8, EMP3, HOXA9, NR1I2* and *CD44*. *CASP8* is an anti-apoptotic gene, and its methylation was reported to be associated with poor survival with HR of 5.3 ($P = 0.008$).[42] Also, methylation of *EMP3, HOXA9, NR1I2* and *CD44* were associated with poor survival with a *P*-value of 0.014, 0.03, 0.04 and 0.049, respectively.[42–45] We found that CIMP was associated with methylation of multiple promoter CGIs, mainly *CASP8* and *NR1I2*, but had stronger prognostic power than methylation of individual genes.[46] These results strengthened the hypothesis that CIMP leads to poor prognosis by induction of methylation of promoter CGIs of various tumor-suppressor genes at low incidences.

## CIMP AS A POTENTIAL TARGET OF EPIGENETIC THERAPY

Poor prognosis of NBLs with CIMP is likely to be caused by silencing of multiple genes due to methylation of their promoter CGIs. As silenced genes are multiple and variable among individual NBLs, it was hypothesized that simultaneous demethylation of multiple genes could be effective for treatment of NBLs (Figure 4). Indeed, treatment of NBL cell lines with a demethylating drug, 5-aza-CdR, enhanced the sensitivity to the differentiation effect by 13-*cis*-retinoic acid.[8]

In addition to CIMP, aberrant histone modifications or modifying enzymes are also emerging as potential therapeutic targets of NBLs. For example, lysine-specific demethylase 1 (LSD1), a histone H3 lysine4 (H3K4) demethylase, is highly expressed in poorly differentiated NBLs, and inhibition of LSD1 using a monoamine oxidase inhibitor, tranylcypromine, resulted in growth suppression of NBLs *in vitro* and *in vivo*.[47] To improve selectivity for LSD1 over monoamine oxidase inhibitor, LSD1-selective inhibitors were developed,[48] and they are expected to show high anticancer efficacy and low toxicity in normal cells.

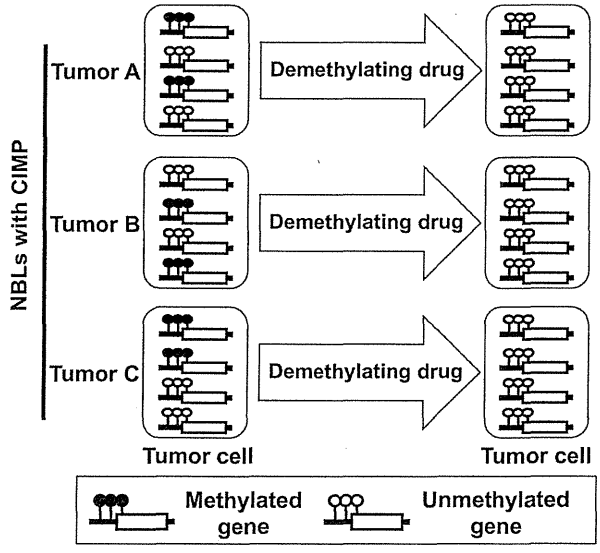


**Figure 4** The concept of demethylating drug treatment for neuroblastomas (NBLs). In individual NBLs (tumor A–C), multiple but different tumor-suppressor genes are methylation-silenced, and reversal of these individual genes is difficult. By the use of a demethylating drug, multiple tumor-suppressor genes become simultaneously demethylated, and NBL cells are expected to show better responses to differentiation and cytotoxic agents.

Clinically, a phase I study of 5-aza-CdR with doxorubicin and cyclophosphamide in children with NBLs and other solid tumors was conducted in the United States,[49] and low-dose 5-aza-CdR ($5\,mg\,m^{-2}$) turned out to have tolerable toxicity in children. However, doses of 5-aza-CdR capable of producing clinically relevant biologic effects were not well tolerated. Different combinations between 5-aza-CdR and other drugs, such as differentiating drugs (13-*cis*-retinoic acid) or other epigenetic drugs (LSD1 inhibitors and histone deacetylase inhibitors), could improve the effectiveness of the demethylating drug for NBLs.

## CONCLUSIONS

The usefulness of aberrant DNA methylation in cancer diagnostics and therapeutics is now coming into practice. In NBLs, CIMP has prognostic power in cases without *MYCN* amplification, and its strong prognostic power was validated in German, Italian and Swedish NBL cases. Combinations of a DNA-demethylating drug with a differentiating drug has been shown to be effective for NBLs with CIMP *in vitro*, and the appropriate dose and appropriate combination is expected to improve survival of NBL cases. Epigenetic diagnosis and therapeutics are becoming or have become an important choice for cancer patients.

## CONFLICT OF INTEREST

The authors declare no conflict of interest.

## ACKNOWLEDGEMENTS

This study was supported by Grants-in-Aid for the Third-Term Cancer Control Strategy Program from the Ministry of Health, Labour and Welfare, Japan, and by the National Cancer Center Research and Development Fund, Japan.

1 Church, T. R., Wandell, M., Lofton-Day, C., Mongin, S. J., Burger, M., Payne, S. R. *et al.* Prospective evaluation of methylated SEPT9 in plasma for detection of asymptomatic colorectal cancer. *Gut* in press (2013).
2 Hegi, M. E., Diserens, A. C., Gorlia, T., Hamou, M. F., de Tribolet, N., Weller, M. *et al.* MGMT gene silencing and benefit from temozolomide in glioblastoma. *N. Engl. J. Med.* **352,** 997–1003 (2005).
3 Van Neste, L., Herman, J. G., Otto, G., Bigley, J. W., Epstein, J. I. & Van Criekinge, W. The epigenetic promise for prostate cancer diagnosis. *Prostate* **72,** 1248–1261 (2011).
4 Teodoridis, J. M., Hardie, C. & Brown, R. CpG island methylator phenotype (CIMP) in cancer: causes and implications. *Cancer Lett.* **268,** 177–186 (2008).
5 Cowan, L. A., Talwar, S., Yang, A. S. & Will, D. N. A. Methylation inhibitors work in solid tumors? A review of the clinical experience with azacitidine and decitabine in solid tumors. *Epigenomics* **2,** 71–86 (2010).
6 Foulks, J. M., Parnell, K. M., Nix, R. N., Chau, S., Swierczek, K., Saunders, M. *et al.* Epigenetic drug discovery: targeting DNA methyltransferases. *J. Biomol. Screen.* **17,** 2–17 (2012).
7 Juergens, R. A., Wrangle, J., Vendetti, F. P., Murphy, S. C., Zhao, M., Coleman, B. *et al.* Combination epigenetic therapy has efficacy in patients with refractory advanced non-small cell lung cancer. *Cancer Discov.* **1,** 598–607 (2011).
8 Abe, M., Watanabe, N., McDonell, N., Takato, T., Ohira, M., Nakagawara, A. *et al.* Identification of genes targeted by CpG island methylator phenotype in neuroblastomas, and their possible integrative involvement in poor prognosis. *Oncology* **74,** 50–60 (2008).
9 Matei, D., Fang, F., Shen, C., Schilder, J., Arnold, A., Zeng, Y. *et al.* Epigenetic resensitization to platinum in ovarian cancer. *Cancer Res.* **72,** 2197–2205 (2012).
10 Toyota, M., Ahuja, N., Ohe-Toyota, M., Herman, J. G., Baylin, S. B. & Issa, J. P. CpG island methylator phenotype in colorectal cancer. *Proc. Natl Acad. Sci. USA* **96,** 8681–8686 (1999).
11 Ogino, S., Nosho, K., Kirkner, G. J., Kawasaki, T., Meyerhardt, J. A., Loda, M. *et al.* CpG island methylator phenotype, microsatellite instability, BRAF mutation and clinical outcome in colon cancer. *Gut* **58,** 90–96 (2009).
12 Shen, L., Toyota, M., Kondo, Y., Lin, E., Zhang, L., Guo, Y. *et al.* Integrated genetic and epigenetic analysis identifies three different subclasses of colon cancer. *Proc. Natl Acad. Sci. USA* **104,** 18654–18659 (2007).
13 Yagi, K., Akagi, K., Hayashi, H., Nagae, G., Tsuji, S., Isagawa, T. *et al.* Three DNA methylation epigenotypes in human colorectal cancer. *Clin. Cancer Res.* **16,** 21–33 (2010).
14 Suzuki, H., Igarashi, S., Nojima, M., Maruyama, R., Yamamoto, E., Kai, M. *et al.* IGFBP7 is a p53-responsive gene specifically silenced in colorectal cancer with CpG island methylator phenotype. *Carcinogenesis* **31,** 342–349 (2010).
15 Hinoue, T., Weisenberger, D. J., Pan, F., Campan, M., Kim, M., Young, J. *et al.* Analysis of the association between CIMP and BRAF in colorectal cancer by DNA methylation profiling. *PLoS One* **4,** e8357 (2009).
16 Kim, H., Kim, Y. H., Kim, S. E., Kim, N. G. & Noh, S. H. Concerted promoter hypermethylation of hMLH1, p16INK4A, and E-cadherin in gastric carcinomas with microsatellite instability. *J. Pathol.* **200,** 23–31 (2003).
17 Toyota, M., Ahuja, N., Suzuki, H., Itoh, F., Ohe-Toyota, M., Imai, K. *et al.* Aberrant methylation in gastric cancer associated with the CpG island methylator phenotype. *Cancer Res.* **59,** 5438–5442 (1999).
18 Marsit, C. J., Houseman, E. A., Christensen, B. C., Eddy, K., Bueno, R., Sugarbaker, D. J. *et al.* Examination of a CpG island methylator phenotype and implications of methylation profiles in solid tumors. *Cancer Res.* **66,** 10621–10629 (2006).
19 Shen, L., Ahuja, N., Shen, Y., Habib, N. A., Toyota, M., Rashid, A. *et al.* DNA methylation and environmental exposures in human hepatocellular carcinoma. *J. Natl Cancer Inst.* **94,** 755–761 (2002).
20 Strathdee, G., Appleton, K., Illand, M., Millan, D. W., Sargent, J., Paul, J. *et al.* Primary ovarian carcinomas display multiple methylator phenotypes involving known tumor suppressor genes. *Am. J. Pathol.* **158,** 1121–1127 (2001).
21 Roman-Gomez, J., Jimenez-Velasco, A., Agirre, X., Castillejo, J. A., Navarro, G., Calasanz, M. J. *et al.* CpG island methylator phenotype redefines the prognostic effect of t(12;21) in childhood acute lymphoblastic leukemia. *Clin. Cancer Res.* **12,** 4845–4850 (2006).
22 Maruyama, R., Toyooka, S., Toyooka, K. O., Harada, K., Virmani, A. K., Zochbauer-Muller, S. *et al.* Aberrant promoter methylation profile of bladder cancer and its relationship to clinicopathological features. *Cancer Res.* **61,** 8659–8663 (2001).
23 Brock, M. V., Gou, M., Akiyama, Y., Muller, A., Wu, T. T., Montgomery, E. *et al.* Prognostic importance of promoter hypermethylation of multiple genes in esophageal adenocarcinoma. *Clin. Cancer Res.* **9,** 2912–2919 (2003).
24 Wei, S. H., Chen, C. M., Strathdee, G., Harnsomburana, J., Shyu, C. R., Rahmatpanah, F. *et al.* Methylation microarray analysis of late-stage ovarian carcinomas distinguishes progression-free survival in patients and identifies candidate epigenetic markers. *Clin. Cancer Res.* **8,** 2246–2252 (2002).
25 Kusano, M., Toyota, M., Suzuki, H., Akino, K., Aoki, F., Fujita, M. *et al.* Genetic, epigenetic, and clinicopathologic features of gastric carcinomas with the CpG island methylator phenotype and an association with Epstein-Barr virus. *Cancer* **106,** 1467–1479 (2006).
26 Noushmehr, H., Weisenberger, D. J., Diefes, K., Phillips, H. S., Pujara, K., Berman, B. P. *et al.* Identification of a CpG island methylator phenotype that defines a distinct subgroup of glioma. *Cancer Cell* **17,** 510–522 (2010).
27 Turcan, S., Rohle, D., Goenka, A., Walsh, L. A., Fang, F., Yilmaz, E. *et al.* IDH1 mutation is sufficient to establish the glioma hypermethylator phenotype. *Nature* **483,** 479–483 (2012).
28 Dang, L., White, D. W., Gross, S., Bennett, B. D., Bittinger, M. A., Driggers, E. M. *et al.* Cancer-associated IDH1 mutations produce 2-hydroxyglutarate. *Nature* **462,** 739–744 (2009).
29 Xu, W., Yang, H., Liu, Y., Yang, Y., Wang, P., Kim, S. H. *et al.* Oncometabolite 2-hydroxyglutarate is a competitive inhibitor of alpha-ketoglutarate-dependent dioxygenases. *Cancer Cell* **19,** 17–30 (2011).
30 Figueroa, M. E., Abdel-Wahab, O., Lu, C., Ward, P. S., Patel, J., Shih, A. *et al.* Leukemic IDH1 and IDH2 mutations result in a hypermethylation phenotype, disrupt TET2 function, and impair hematopoietic differentiation. *Cancer Cell* **18,** 553–567 (2010).
31 Maris, J. M. Recent advances in neuroblastoma. *N. Engl. J. Med.* **362,** 2202–2211 (2010).
32 Cohn, S. L., Pearson, A. D., London, W. B., Monclair, T., Ambros, P. F., Brodeur, G. M. *et al.* The International Neuroblastoma Risk Group (INRG) classification system: an INRG Task Force report. *J. Clin. Oncol.* **27,** 289–297 (2009).
33 Jaenisch, R. & Bird, A. Epigenetic regulation of gene expression: how the genome integrates intrinsic and environmental signals. *Nat. Genet.* **33** (Suppl), 245–254 (2003).
34 Li, E. Chromatin modification and epigenetic reprogramming in mammalian development. *Nat. Rev. Genet.* **3,** 662–673 (2002).
35 Abe, M., Ohira, M., Kaneda, A., Yagi, Y., Yamamoto, S., Kitano, Y. *et al.* CpG island methylator phenotype is a strong determinant of poor prognosis in neuroblastomas. *Cancer Res.* **65,** 828–834 (2005).
36 Abe, M., Westermann, F., Nakagawara, A., Takato, T., Schwab, M. & Ushijima, T. Marked and independent prognostic significance of the CpG island methylator phenotype in neuroblastomas. *Cancer Lett.* **247,** 253–258 (2007).
37 Banelli, B., Brigati, C., Di Vinci, A., Casciano, I., Forlani, A., Borzi, L. *et al.* A pyrosequencing assay for the quantitative methylation analysis of the PCDHB gene cluster, the major factor in neuroblastoma methylator phenotype. *Lab. Invest.* **92,** 458–465 (2011).
38 Kiss, N. B., Kogner, P., Johnsen, J. I., Martinsson, T., Larsson, C. & Geli, J. Quantitative global and gene-specific promoter methylation in relation to biological properties of neuroblastomas. *BMC Med. Genet.* **13,** 83 (2012).
39 Schwab, M., Alitalo, K., Klempnauer, K. H., Varmus, H. E., Bishop, J. M., Gilbert, F. *et al.* Amplified DNA with limited homology to myc cellular oncogene is shared by human neuroblastoma cell lines and a neuroblastoma tumour. *Nature* **305,** 245–248 (1983).

40 Brodeur, G. M., Seeger, R. C., Schwab, M., Varmus, H. E. & Bishop, J. M. Amplification of N-myc in untreated human neuroblastomas correlates with advanced disease stage. *Science* **224,** 1121–1124 (1984).
41 Seeger, R. C., Brodeur, G. M., Sather, H., Dalton, A., Siegel, S. E., Wong, K. Y. *et al.* Association of multiple copies of the N-myc oncogene with rapid progression of neuroblastomas. *N. Engl. J. Med.* **313,** 1111–1116 (1985).
42 Grau, E., Martinez, F., Orellana, C., Canete, A., Yanez, Y., Oltra, S. *et al.* Hypermethylation of apoptotic genes as independent prognostic factor in neuroblastoma disease. *Mol. Carcinog.* **50,** 153–162 (2011).
43 Alaminos, M., Davalos, V., Ropero, S., Setien, F., Paz, M. F., Herranz, M. *et al.* EMP3, a myelin-related gene located in the critical 19q13.3 region, is epigenetically silenced and exhibits features of a candidate tumor suppressor in glioma and neuroblastoma. *Cancer Res.* **65,** 2565–2571 (2005).
44 Alaminos, M., Davalos, V., Cheung, N. K., Gerald, W. L. & Esteller, M. Clustering of gene hypermethylation associated with clinical risk groups in neuroblastoma. *J. Natl Cancer Inst.* **96,** 1208–1219 (2004).
45 Misawa, A., Inoue, J., Sugino, Y., Hosoi, H., Sugimoto, T., Hosoda, F. *et al.* Methylation-associated silencing of the nuclear receptor 1I2 gene in advanced-type neuroblastomas, identified by bacterial artificial chromosome array-based methylated CpG island amplification. *Cancer Res.* **65,** 10233–10242 (2005).
46 Asada, K., Watanabe, N., Nakamura, Y., Ohira, M., Westermann, F., Scwab, M. *et al.* Stronger prognostic power of the CpG island methylator phenotype than methylation of individual genes in neuroblastomas. *Jpn J. Clin. Oncol.* in press (2013).
47 Schulte, J. H., Lim, S., Schramm, A., Friedrichs, N., Koster, J., Versteeg, R. *et al.* Lysine-specific demethylase 1 is strongly expressed in poorly differentiated neuroblastoma: implications for therapy. *Cancer Res.* **69,** 2065–2071 (2009).
48 Ueda, R., Suzuki, T., Mino, K., Tsumoto, H., Nakagawa, H., Hasegawa, M. *et al.* Identification of cell-active lysine specific demethylase 1-selective inhibitors. *J. Am. Chem. Soc.* **131,** 17536–17537 (2009).
49 George, R. E., Lahti, J. M., Adamson, P. C., Zhu, K., Finkelstein, D., Ingle, A. M. *et al.* Phase I study of decitabine with doxorubicin and cyclophosphamide in children with neuroblastoma and other solid tumors: a Children's Oncology Group study. *Pediatr. Blood Cancer* **55,** 629–638 (2010).
50 Weisenberger, D. J., Siegmund, K. D., Campan, M., Young, J., Long, T. I., Faasse, M. A. *et al.* CpG island methylator phenotype underlies sporadic microsatellite instability and is tightly associated with BRAF mutation in colorectal cancer. *Nat. Genet.* **38,** 787–793 (2006).

*Published online 12 June 2013*

*Nucleic Acids Research, 2013, Vol. 41, No. 15 7231–7239*
*doi:10.1093/nar/gkt528*

# Visualization of multivalent histone modification in a single cell reveals highly concerted epigenetic changes on differentiation of embryonic stem cells

**Naoko Hattori[1], Tohru Niwa[1], Kana Kimura[1], Kristian Helin[2,3] and Toshikazu Ushijima[1,*]**

[1]Division of Epigenomics, National Cancer Center Research Institute, 5-1-1 Tsukiji, Chuo-ku, Tokyo 104-0045, Japan, [2]Biotech Research and Innovation Centre (BRIC), University of Copenhagen, Ole Maaløes Vej 5, 2200 Copenhagen, Denmark and [3]Centre for Epigenetics, University of Copenhagen, Ole Maaløes Vej 5, 2200 Copenhagen, Denmark

Received December 6, 2012; Revised May 19, 2013; Accepted May 22, 2013

## ABSTRACT

**Combinations of histone modifications have significant biological roles, such as maintenance of pluripotency and cancer development, but cannot be analyzed at the single cell level. Here, we visualized a combination of histone modifications by applying the *in situ* proximity ligation assay, which detects two proteins in close vicinity (~30 nm). The specificity of the method [designated as imaging of a combination of histone modifications (iChmo)] was confirmed by positive signals from H3K4me3/acetylated H3K9, H3K4me3/RNA polymerase II and H3K9me3/H4K20me3, and negative signals from H3K4me3/H3K9me3. Bivalent modification was clearly visualized by iChmo in wild-type embryonic stem cells (ESCs) known to have it, whereas rarely in *Suz12* knockout ESCs and mouse embryonic fibroblasts known to have little of it. iChmo was applied to analysis of epigenetic and phenotypic changes of heterogeneous cell population, namely, ESCs at an early stage of differentiation, and this revealed that the bivalent modification disappeared in a highly concerted manner, whereas phenotypic differentiation proceeded with large variations among cells. Also, using this method, we were able to visualize a combination of repressive histone marks in tissue samples. The application of iChmo to samples with heterogeneous cell population and tissue samples is expected to clarify unknown biological and pathological significance of various combinations of epigenetic modifications.**

## INTRODUCTION

Histone modifications are known to play important roles in various biological and pathological processes, such as cell type-specific gene expression and cancer development (1,2). In addition, the crucial importance of their combinations is indicated by recent findings, such as the presence of cell type-specific multivalent histone modifications revealed by genome-wide analyses (3–7) and proteins that recognize a combination of histone modifications (8). Especially, the combination of histone H3 lysine 4 trimethylation (H3K4me3) and histone H3 lysine 27 trimethylation (H3K27me3), named the bivalent modification, is present almost exclusively in pluripotent stem cells, such as embryonic stem cells (ESCs) (3,5), early stage embryos (9) and immature T-cells (10), and is thought to maintain the 'stemness' of these cells. Furthermore, aberrant expression of a protein that binds to a specific combination of histone modifications was associated with poor prognosis in breast cancer, suggesting the importance of a combination also in pathological processes (11).

Regardless of the crucial importance of combinations of histone modifications, methodologies to detect combinations are so far limited to the sequential-chromatin immunoprecipitation (sequential-ChIP) assay (3,12) and recently developed immunoprecipitation-mass spectrometry assay (13). Although a sequential-ChIP assay has the advantage to identify genomic regions with a specific combination of histone modifications, it suffers from the necessity of a large number of cells, and its application is limited to samples containing $>10^6$ cells. Moreover, in samples with heterogeneous cell populations, it is impossible to identify cells with a specific combination of histone modifications. Owing to this limitation, we cannot identify which cells have a specific multivalent

*To whom correspondence should be addressed. Tel: +81 3 3547 5240; Fax: +81 3 5565 1753; Email: tushijim@ncc.go.jp

modification in samples derived from tissues, and even in a cell line if the sample consists of cells at various differentiation stages.

In this study, we aimed to visualize the coexistence of two histone modifications by applying the *in situ* proximity ligation assay (*in situ* PLA), an imaging technique of protein–protein interactions (14). Based on the principle of *in situ* PLA, if two different modifications recognized by respective first antibodies exist approximately within 30 nm, oligonucleotide probes conjugated to their secondary antibodies can serve as a template for rolling-circle amplification. The amplification products can hybridize with fluorescent probes and be detected as fluorescence signals, reflecting the combination of histone modifications. In addition, we applied the method to analyze the presence of a specific combination of histone modifications in heterogeneous cell populations and tissue sections.

## MATERIALS AND METHODS

### Culture of mouse ESCs and embryonic fibroblasts

J1 ESC line and *Suz12* knockout (KO) ESC line (clone SBE8) established as reported (15) were cultured in normal ESC medium with 15% fetal bovine serum and 1000 U/ml of leukemia inhibitory factor (LIF) (ESGRO, Chemicon, CA) on mitotically inactivated mouse embryonic fibroblasts (MEFs) kindly provided by Dr Shiota K. (The University of Tokyo). For immunofluorescence staining and imaging of a combination of histone modifications (iChmo), MEFs at passage three were purchased from Millipore (Billerica, MA) and cultured in Dulbecco's modified Eagle's medium with 10% fetal bovine serum for 6 days at passage five. To induce differentiation of ESCs, cells were seeded on 0.1% gelatin-coated cell plate at a density of $3.0 \times 10^5$ cells/100 mm dish in the absence of feeder layer cells and LIF and then pre-cultured for 1 day. After pre-culture, ESCs were cultured for 24 or 48 h with 1 μM of all-trans retinoic acid (RA) (Sigma, St. Louis, MO). The medium was changed every day.

### Preparation of mouse and human tissue samples

For RNA extraction, mouse liver and brain were resected from 8-week-old C57BL/6J male mice purchased from CLEA Japan, Inc. (Tokyo, Japan). For preparation of histological sections, human colonic tissues resected with a colon cancer were obtained, embedded in Tissue-Tek O.C.T. Compound (Sakura Finetek Japan, Tokyo, Japan) and frozen on dry ice. Sections of 4 μm of thickness were prepared for immunofluorescence staining and iChmo without a dry step. The animal experiments were approved by the Committee for Ethics in Animal Experimentation at the National Cancer Center. Human samples were obtained with informed consent, and the analysis was approved by the institutional review boards.

### Immunofluorescence staining

For immunofluorescence staining, cells and tissue sections were fixed with 4% formaldehyde for 15 min, washed three times in PBS and permeabilized by 1% Triton X-100 in PBS for 20 min. After washing five times in PBS, cells and sections were incubated in blocking buffer (1% BSA in PBS) for 30 min and then with mouse monoclonal antibodies directed against H3K4me3 (1:1000; Wako, Tokyo, Japan; 307-34813), H4K20me3 (1:1000; Abcam, Cambridge, MA; ab78517), Oct-3/4 (1:500; Santa Cruz Biotechnology, Santa Cruz, CA; sc-5279) or ßIII-tubulin (1:500; Covance, Berkeley, CA; MMS-435P), or with rabbit polyclonal antibodies directed against acetylated H3K9 (H3K9ac) (1:500, Abcam; ab10812), H3K9me3 (1:1000, Millipore: 07-442), H3K27me3 (1:1000, Millipore; 07-449) or RNA polymerase II (RNAPII) (1:500, Abcam; ab5095) in the same buffer for 1 h. The specificity of antibodies against histone modifications was confirmed previously (16,17). Cells and sections were washed in PBS three times for 5 min and incubated in Alexa Fluor 594-conjugated goat anti-rabbit IgG (1:1000, Invitrogen, Carlsbad, CA) or Alexa Fluor 488-conjugated goat anti-mouse IgG (1:1000, Invitrogen) for 1 h. After washing with PBS three times for 5 min, coverslips were mounted using ProLong Gold antifade reagent with 4′,6-diamidino-2-phenylindole (DAPI) (Invitrogen). Fluorescence of cultured cells stained with histone modification antibodies was detected under a laser-scanning confocal microscope (LSM710; Carl Zeiss, Oberkochen, Germany), and all images were acquired and analyzed using LSM Software ZEN 2008 (Carl Zeiss). Images of Oct-4 and ßIII-tubulin staining of ESCs and of human tissue sections were captured using a FV10iW laser-scanning confocal microscope (Olympus, Tokyo, Japan).

### iChmo

Duolink *in situ* PLA was purchased from Olink Bioscience (Uppsala, Sweden). First, cells and tissue sections were fixed, permeabilized and incubated with primary antibodies under the same condition in the immunofluorescence staining. The primary antibodies were the same as those for the immunofluorescence staining, and the concentrations were two times higher than those for the immunofluorescence staining. Then, samples were incubated with secondary antibodies conjugated with PLA probes MINUS and PLUS at 37°C for 90 min. Finally, the PLA probes MINUS and PLUS were ligated using two connecting oligonucleotides to produce a template for rolling-cycle amplification. After amplification, the amplification products were hybridized with red fluorescence-labeled oligonucleotide. Samples were mounted on coverslips using ProLong Gold antifade reagent with DAPI. Fluorescence of cultured cells was detected under LSM710, and all images were acquired and analyzed using ZEN 2008. For quantitative analysis of iChmo signals, the fluorescence spots were counted using Z-stack acquisition of BZ-9000 microscope system. Fluorescence of tissue sections was captured using a FV10iW laser-scanning confocal microscope.

### Quantitative reverse transcription-PCR

DNase-treated total RNA (1 μg) was reverse-transcribed with Oligo-$dT_{20}$ (Invitrogen, Carlsbad, CA) and Superscript III reverse transcriptase (Invitrogen).

Quantitative PCR (qPCR) was carried out by real-time PCR using SYBR® Green I. The primer sequences and PCR conditions are shown in Supplementary Table S1. The amplification curve of a sample was compared with those of standard DNA samples with known copy numbers to obtain the copy number in the sample. The number of target cDNA molecules was normalized to those of mouse *Gapdh* cDNA molecules.

### Statistical analysis

To evaluate significant difference between two independent groups of sample data, the Mann–Whitney *U*-test was used.

## RESULTS

### Combinations of epigenetic marks are visualized by iChmo

To visualize a combination of histone modifications, we first performed the *in situ* PLA focusing on two combinations of epigenetic marks known to be present at active loci, one H3K4me3 and H3K9ac and the other H3K4me3 and RNAPII (18). Immunofluorescence staining of mouse ESCs confirmed that the signals of H3K4me3 and H3K9ac, and those of H3K4me3 and RNAPII, were observed as merged signals in the nucleus (Figure 1A and B). The *in situ* PLA for the combinations of H3K4me3/H3K9ac and H3K4me3/RNAPII demonstrated a large number of fluorescence spots in the nucleus (Figure 1E and F). The possibility that the signals were derived from non-specific binding of PLA probes was excluded by the absence of fluorescence spots of the *in situ* PLA using antibodies against H3K4me3 and H3K9me3 that were not merged by immunofluorescence (Figure 1D and H). Quantitatively, the mean number of spots of H3K4me3/H3K9ac, H3K4me3/RNAPII and H3K4me3/H3K9me3 was 22.9, 25.9 and 2.4 per nucleus, respectively (Figure 1I). Therefore, the coexistence of epigenetic marks was visualized at the single cell level by applying the *in situ* PLA, and this method was designated as iChmo.

Next, we analyzed whether iChmo can also detect a combination of two marks at a different histone protein of the same or neighboring nucleosomes within 30 nm, such as H3 and H4. By immunofluorescence using antibodies against H3K9me3 and H4K20me3, epigenetic marks for heterochromatin, their colocalization was confirmed by the presence of merged signals (Figure 1C). By iChmo using the same two antibodies, a large number of spots were produced (Figure 1G), and the mean number of spots was 72.5 per nucleus (Figure 1I), indicating that iChmo can visualize a combination of epigenetic marks, even if they are at different histone proteins in a close proximity.

### Bivalent modification is specifically visualized at the single cell level

We focused on bivalent modification because of its biological significance and applied iChmo to visualize it using mouse ESCs and MEFs that have a lot of and few, respectively, bivalent modifications (3,5). By immunofluorescence staining of ESCs, H3K4me3 signals were observed as interspersed small dots, whereas H3K27me3 signals were enriched at the periphery of the nuclear membrane (Figure 2A). Some signals were merged in the nucleus, appearing to reflect the presence of bivalent modification. However, the same staining pattern was observed in MEFs (Supplementary Figure S1), and it was shown that immunofluorescence was not capable of distinguishing whether H3K4me3 and H3K27me3 were in close proximity. However, notably, by iChmo, a large number of fluorescence spots were observed in ESCs, whereas only a small number of spots were in MEFs (Figure 2B). This demonstrated that iChmo can distinguish whether two modifications coexist in the vicinity at the single cell level.

### iChmo signals of bivalent modification are decreased in MEFs and Suz12 KO ESCs

To further confirm that iChmo signals originated from bivalent modification, we performed iChmo using *Suz12* KO ESCs. Suz12 is a component of Polycomb repressive complexes 2 together with Ezh2 and Eed (19), and is required for Polycomb repressive complexes 2 enzymatic activity (20). In the *Suz12* KO ESCs, global loss of H3K27me3 was observed by western blotting (15) and by immunofluorescence (Supplementary Figure S1), and loss of genomic regions with bivalent modification by quantitative ChIP-PCR (Supplementary Figure S2). iChmo produced no or few fluorescence spots of bivalent modification in the nucleus of *Suz12* KO ESCs (Figure 2B). The fact that this technique itself worked even in *Suz12* KO ESCs and MEFs was confirmed by detecting the coexistence of H3K4me3/H3K9ac and H3K4me3/RNAPII in these cells (Supplementary Figure S3). Quantitatively, the mean number of spots from bivalent modification was 0.9 and 4.1 per nucleus in the *Suz12* KO ESCs (69 nuclei counted) and MEFs (60 nuclei counted), respectively, whereas it was 15.2 in wild-type (WT) ESCs (58 nuclei counted) (Figure 2C). These data clearly showed that application of iChmo enabled us to visualize the bivalent modifications at the single cell level.

### iChmo reveals highly concerted epigenetic changes during ESC differentiation

We took advantage of an imaging method to analyze individual cells in a heterogeneous sample, namely, ESCs at an early stage of differentiation. ESC differentiation was induced by all-trans RA treatment 24 h after removal of LIF and feeder layer cells. The expression of *Oct-4* mRNA decreased to the half 24 h after the RA treatment, but was still detectable 48 h after the treatment (Figure 3A). At cellular level, Oct-4 protein was detectable in all ESCs before the treatment but was heterogeneously detectable 24 h later (Figure 3B). At 48 h, in accordance with the residual *Oct-4* mRNA expression, a minor fraction of ESCs still had the Oct-4 protein expression (Figure 3B). ßIII-tubulin, a differentiated neuron marker, was also expressed in only a fraction of the ESCs (Figure 3B), showing the presence of large variations in the phenotypic

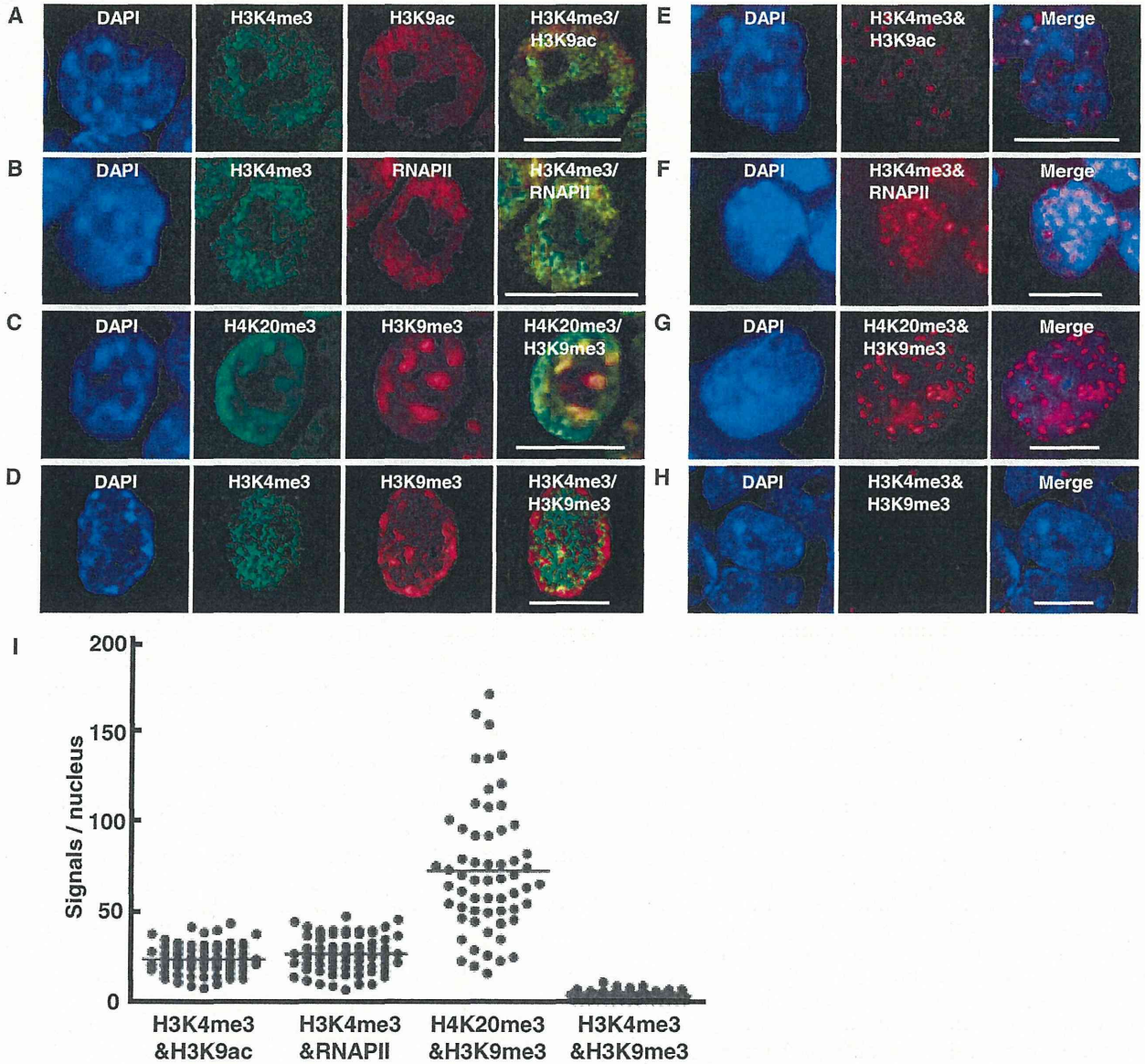


**Figure 1.** Visualization of combinations of epigenetic modifications in a single cell. Immunofluorescence staining was performed using mouse ESCs and antibodies against H3K4me3 and H3K9ac (**A**), H3K4me3 and RNAPII (**B**), H4K20me3 and H3K9me3 (**C**) and H3K4me3 and H3K9me3 (**D**). Colocalizations of H3K4me3/H3K9Ac, of H3K4me3/RNAP2 and of H4K20me3/H3K9me3 were observed, whereas that of H3K4me3/H3K9me3 was not. iChmo was performed using mouse ESCs and antibodies against H3K4me3 and H3K9ac (**E**), H3K4me3 and RNAPII (**F**), H4K20me3 and H3K9me3 (**G**) and H3K4me3 and H3K9me3 (**H**). Coexistence of H3K4me3/H3K9ac, of H3K4me3/RNAPII and of H4K20me3/H3K9me3, but not of H3K4me3/H3K9me3, was observed. Scale bar represents 10 μm. (**I**) The number of iChmo spots was counted for individual combinations in the nuclei of ESCs (H3K4me3 and H3K9ac, $n = 71$; H3K4me3 and RNAPII, $n = 70$; H4K20me3 and H3K9me3, $n = 60$; and H3K4me3 and H3K9me3, $n = 80$).

differentiation of the ESCs. In contrast, no or little fluorescence spots of the bivalent modification were observed 24 and 48 h after the RA treatment by iChmo, regardless of whether ESCs formed colonies or were differentiated into neuron-like cells (Figure 3C). The mean number of spots of ESCs at 48 h after the RA treatment was at the same level as that of the *Suz12* KO ESCs (Figure 3D). These data indicated that the epigenetic layer of differentiation was completed at 2 days in a highly concerted manner, whereas the phenotypic layer of differentiation proceeded with considerable variation.

### iChmo visualizes a combination of histone modifications in tissue samples

If histone combinations in individual cells can be analyzed in tissues, this will enable us to identify cell populations of unique functions, such as stem cells. To apply iChmo to a